Revised manuscript: AEM01841-21

Mbn C is not required for the formation of the N-terminal oxazolone in the methanobactin from *Methylosinus trichosporium* OB3b.

Philip Dershwitz[1,Ψ], Wenyu Gu[2Ψ‡], Julien Roche[1], Christina S. Kang-Yun[2†],Jeremy D. Semrau[2], Thomas A. Bobik[1], Bruce Fulton[1], Hans Zischka[3], and Alan A. DiSpirito[1]*

[1]Roy J. Carver Department of Biochemistry, Biophysics and Molecular Biology. Iowa State University, Ames, IA 50011-3260, USA

[2]Department of Civil and Environmental Engineering, University of Michigan, Ann Arbor, MI, 48109-2125, USA

[3]Institute of Molecular Toxicology and Pharmacology, Helmholtz Center Münich, German Research Center and Environmental Health, Ingolsteadter Landstrasse, Germany and Technical University Münich, School of Medicine, Institute of Toxicology and Environmental Hygiene, Biedersteiner Strasse 29, D-80802 Munich, Germany.

[Ψ]Co-first authors

[‡]Current address: Department of Civil & Environmental Engineering, Stanford University, Stanford, CA, 94305, USA

[†]Current address: Biosciences and Biotechnology Division, Lawrence Livermore National Laboratory, Livermore, CA, 94550-9698, USA

*To whom correspondence should be addressed: Email: aland@iastate.edu; Phone: 1-515-294-2944; Fax: 1-515-294-0453

Running title: Role of MbnC in Methanobactin Biosynthesis

ABSTRACT Methanobactins (MBs) are ribosomally synthesized and post-translationally modified peptides (RiPPs) produced by methanotrophs for copper uptake. The post-translational modification that define MBs is the formation of two heterocyclic groups with associated thioamines from X-Cys dipeptide sequences. Both heterocyclic groups in the MB from *Methylosinus trichosporium* OB3b (MB-OB3b) are oxazolone groups. The precursor gene for MB-OB3b, *mbnA*, which is part of a gene cluster that contains both annotated and unannotated genes. One of those unannotated genes, *mbnC*, is found in all MB operons, and in conjunction with *mbnB*, is reported to be involved in the formation of both heterocyclic groups in all MBs. To determine the function of *mbnC*, a deletion mutation was constructed in *M. trichosporium* OB3b, and the MB produced from the Δ*mbn*C mutant was purified and structurally characterized by UV-visible absorption spectroscopy, mass spectrometry and solution NMR spectroscopy. MB-OB3b from Δ*mbn*C was missing the C-terminal Met and also found to contain a Pro and a Cys in place of the pyrrolidiny-oxazolone-thioamide group. These results demonstrate MbnC is required for the formation of the C-terminal pyrrolidinyl-oxazolone-thioamide group from the Pro-Cys dipeptide, but not for the formation of the N-terminal 3-methylbutanol-oxazolone-thioamide group from the N-terminal dipeptide Leu-Cys.

IMPORTANCE A number of environmental and medical applications have been proposed for MBs, including bioremediation of toxic metals, nanoparticle formation, as well as for the treatment of copper- and iron-related diseases. However, before MBs can be modified and optimized for any specific application, the biosynthetic pathway for MB production must be defined. The discovery that *mbnC* is involved in the formation of the C-terminal oxazolone

group with associated thioamide but not for the formation of the N-terminal oxazolone group with associated thioamide in *M. trichosporium* OB3b suggests the enzymes responsible for post-translational modification(s) of the two oxazolone groups are not identical.

KEYWORDS methanobactin • chalkophore• methanotroph • aerobic methane oxidation • ribosomally synthesized and posttranslational modified peptide

Methanobactins (MBs) are low molecular mass (<1,300 Da), post-translationally modified copper binding peptides excreted by some methanotrophs as the extracellular component of a copper acquisition system (1-7). Structurally MBs are characterized by the presence of a C-terminal oxazolone group with a C2-associated thioamide and by the presence of an N-terminal oxazolone, imidazolone or pyrazinedione group with an associated thioamide. Some MBs also contain a sulfate group in-place of the hydroxyl group on a Tyr adjacent to the C-terminal oxazolone group. The best characterized MB is from *Methylosinus trichosporium* OB3b and the post-translational modifications for this MB involves: (1) deamination of the N-terminal Leu, (2) conversion of the N-terminal Leu-Cys dipeptide to 1-(N-(mercapto-(5-oxo-2- (3-methylbutanoyl)oxazol-(Z)-4-ylidene)methyl), (3) conversion of the C-terminal Pro-Cys dipeptide into pyrrolidin-2-yl-(mercapto-(5-oxo-oxazol-(Z)-4- ylidene)methyl); and (4) cleavage of the leader sequence (2, 4, 5, 8-11).

The gene encoding the MB precursor peptide, *mbnA*, (5, 10) is found in a gene cluster that contains both genes of known function such as *mbnB* (5, 11), *mbnN* (9), *mbn*T (12) as well as unannotated genes such as *mbnC* (5, 10, 11, 13, 14). MbnB is a member of TIM barrel family as well as the DUF692 family of diiron enzymes (11, 14). In heterologous expression studies in *Escherichia coli*, MbnBC was shown to catalyze a dioxygen-dependent four electron oxidation of Pro-Cys in MbnA (11, 14, 15). The role(s) of MbnB and MbnC could not be separately determined as attempts to separately purify these gene products in *E. coli* failed (11). From these data, it has been argued that MbnBC must act in concert and by doing so create both heterocyclic groups in MBs (11). Such conclusions, however, appear to be premature for several reasons. First, the reported spectra (11) only shows the presence of the C-terminal oxazolone

group, not the N-terminal oxazolone group as the 394 nm absorption maximum is missing. Second, the absorption maximum at 302 nm, diagnostic for the presence of N-terminal oxazolone group was absent (5, 8, 16). Third, no structural data was provided to support the presence of both oxazolone groups. To examine if MbnBC act in concert and are involved in the formation of both oxazolone groups in *M. trichosporium* OB3b, a deletion mutation for MnbC was constructed *(*Δ*mbn*C). The results show MbnC is required for the formation of the C-terminal oxazolone group, but not for the formation of the N-terminal oxazolone group.

RESULTS

Generation of Δ*mbn*C

The Δ*mbnAN* strain previously constructed whereby *mbnABCMN* were deleted using a sucrose counter selected technique (9), was back complemented with *mbnABMN* through selective amplification and ligation of *mbnAB* with *mbnMN*, deleting *mbnC*, and inserting this ligation product into pTJS140, creating pWG104 (Table 1). Successful removal of *mbnC* from this product was confirmed via sequencing (data not shown). The native σ^{70}-dependent promoter upstream of *mbnA* was also incorporated into pWG104, and expression of *mbnABMN* but not *mbnC* (from pWG104), as well as *mbnPH* (from the chromosome) was confirmed via RT-PCR (Figs. S1 and S2).

UV-visible absorption and mass spectrometry of metal-free MB from *M. trichosporium* OB3b *ΔmbnC*

Comparison of the UV-visible absorption spectra of MB from *M. trichosporium* OB3b *ΔmbnC* to wildtype MB-OB3b suggested the of presence of the N-terminal oxazolone group, but the absence of C-terminal oxazolone (Figs. 1 and S3). The molecular mass of native,

full length MB-OB3b is 1154 Da, and MB-OB3b lacking the C-terminal Met is 1023 Da. It should be noted that both forms of MB-OB3b are present in most MB-OB3b preparations (2, 5, 17). The molecular mass of ΔMbnC was 1,018Da as determined by electrospray ionization (ESI) MS/MS (Fig. 2), which was within 1Da of the predicted molecular mass of MB-OB3b in which only one oxazolone group was formed. Taken together, the UV-visible absorption spectra and molecular mass data suggest Δ*mbn*C lacked the C-terminal Met as well as the N-terminal oxazolone group with a 1-(*N*-[mercapto-(5-oxo-2-(3-methylbutanoyl)oxazol-(*Z*)-4-ylidene)methyl]-GSCYPCSC predicted structure (Fig. 3B). In contrast to wild-type MB-OB3b, the C-terminal Met was never observed in MbnC.

Chemical Structure of metal free Δ*mbn*C as determined by NMR spectroscopy. Metal-free MB has multiple conformations, making structural studies of MBs via solution NMR or crystallography difficult (Fig. S4). In prior structural studies of MB, the addition of Cu^{2+} (which is bound and reduced to Cu^{1+} by native MB-OB3b) stabilizes MB-OB3b into one conformation, allowing for crystal formation and NMR characterization (Fig. S4) (2-5, 8, 18). Our initial efforts to investigate the structure of the MB intermediate produced by the Δ*mbn*C strain via NMR were unsuccessful. In contrast to native MB, the MB intermediate from the Δ*mbn*C strain bound, but did not reduce Cu^{2+} to Cu^{+}, resulting in peak broadening from paramagnetic Cu^{2+}. This necessitated a different strategy. Substituting other metals with similar binding behavior for copper, Au^{3+}, Zn^{2+}, Co^{2+} and Ni^{2+} also failed to produce well-behaved complexes. Therefore, it was necessary to examine metal-free Δ*mbn*C.

115 At standard temperature and pressure, Δ*mbn*C undergoes exchange between multiple
116 conformations on an intermediate time scale, leading to excessive line broadening (Fig. S5). In
117 order to slow down the rate of exchange and reduce line broadening, we sampled various
118 temperature and hydrostatic pressure conditions. We found that 2D ^{1}H-^{15}N NMR spectra of
119 Δ*mbn*C recorded at high pressure (3000 bar) and low temperature (265 K) (18,19) show
120 significantly reduced line broadening and gave excellent spectra in the absence of copper (Fig.
121 4).

122 A series of NMR experiments were conducted on Δ*mbn*C, including homonuclear
123 correlation spectroscopy (COSY), total correlation spectroscopy (TOCSY), rotating-frame nuclear
124 Overhauser effect spectroscopy (ROESY), ^{1}H-^{15}N and ^{1}H-^{13}C heteronuclear single-quantum
125 correlation spectroscopy (HSQC), and heteronuclear multiple-bond correlation spectroscopy
126 (HMBC). These experiments enabled assigning all non-hydroxyl ^{1}H, non-conjugated ^{13}C, and all
127 ^{15}N resonances (Table 2 and Figs.4 and S6). The assigned chemical shifts show that the MB from
128 Δ*mbn*C contains 8 amino acids - 3Cys, 2Ser, 1Gly, 1Tyr and 1Pro and 1 oxazolone group (Fig. 4).
129 The 1D ^{15}N experiment showed a peak at 109ppm that was absent from the [^{1}H, ^{15}N]-HSQC
130 spectra and was assigned to proline. However, the glycine nitrogen peak was especially broad,
131 and could only be assigned with the ^{1}H-^{15}N-HSQC. Finally, while the 1D ^{15}N experiment had
132 several resonances around 180ppm - likely due to hydrolysis and deprotonation - only one of
133 them had a correlation with ^{1}H in the ^{1}H-^{15}N-HSQC indicating a single oxazolone group. The
134 NMR results are consistent with the UV-visible absorption spectra, and the ESI-MS results and
135 with the structure shown in Fig. 3B.

DISCUSSION

Due to the variability in the core sequences of structurally characterized MBs, it is difficult to use *mbnA* to screen the potential ability of microbes to produce MB. Instead, *mbnB* and *mbn*C sequences are commonly used as they are found in all known *mbn* gene clusters (5, 13). All known MBs contain two heterocyclic rings, with the N-terminal ring found to be either an oxazolone, pyrazinedione or imidazolone ring, while the C-terminal ring always found to be an oxazolone. Given these data, it could be presumed that MbnBC is involved in the formation of the C-terminal oxazolone group along with an associated thioamide, while the N-terminal oxazolone groups is formed via a different process such as the involvement of an aminotransferase as concluded earlier (5, 9, 10, 13).

Other researchers have attempted to elucidate the role of MbnB and MbnC in methanobactin maturation (11). These individuals were unable to separately heterologously express soluble protein from either MbnB or MbnC , but were able to co-heterologously expressed MbnBC as a heterodimeric complex. In studies where the MbnA precursor polypeptide was incubated with this MbnBC complex, the authors conclude that MbnBC was involved in the formation of both oxazolone groups and the associated thioamides of MB-OB3b. It should be noted, however, that in this study, no structural evidence (i.e., solution NMR data) was provided to definitively show the presence of either ring, rather such conclusions were largely based on mass spectral analyses of MbnA after incubation with the MbnBC complex. Further, the authors assumed that since their construct did not contain the N-terminal aminotransferase, MbnN, the extended conjugation resulting from this reaction would result in both oxazolone groups having identical absorption maxima. The idea that the extended

158 conjugation of the N-terminal oxazolone could be responsible for the bathochromic shift was
159 first proposed as a possible reason for the 50nm shift in the absorption maxima by Krentz *et al.*
160 (5). Kenny *et al*. used this theory to bolster their claim that both oxazolone groups were
161 present in the product from their heterologous system, with both oxazolone groups showing
162 the identical absorption spectra (11). The evidence to support this claim came from their
163 *ΔmbnN* strain in *M. trichosporium* OB3b. MbnN is responsible for the deamination of the N-
164 terminal Leu in *M. trichosporium* OB3b extending the conjugation one additional double bond.
165 In this study the authors claim they can stabilize the MB produced by the *ΔmbnN* strain by the
166 addition of copper before purification. UV-visible absorption spectra of copper containing-
167 ΔMbnN suggest the possible presence of two-oxazolone groups but additional evidence no
168 additional evidence was provided supporting this claim.
169 This observation was surprising as the MB produced by *ΔmbnN* strain in our laboratory
170 showed similar UV-visible absorption spectra throughout the growth cycle suggesting the
171 absence of the N-terminal oxazolone group (Fig. S7). In addition, the UV-visible absorption
172 spectra, LC-MS/MS, FT-ICR-MS, amino acid analysis, number of thiol groups, copper binding
173 properties, and pattern of acid hydrolysis demonstrate the absence of the N-terminal
174 oxazolone group in ΔMbnN (9).
175 Additional evidence that the bathochromic shift in MBs with two oxazolone groups is
176 unlikely to solely arise from the addition of one double bond following deamination of the N-
177 terminal amine comes from examination of the group I MB from *Methylocystis parvus* OBBP.
178 Acid hydrolysis of the MB from *M. parvus* OBBP shows a similar hydrolysis pattern to that
179 observed with the MB from *M. trichosporium* OB3b, demonstrating the presence of two

oxazolone groups, with absorption maxima at 340 and 390nm (Fig. S8). However, both MB operons from *M. parvus* OBBP lack *mbnN* and without deamination of the N-terminal Phe, the conjugation around the N-terminal oxazolone group would not be extended. It is possible that another aminotransferase in the *M. parvus* OBBP genome may catalyze deamination of the N-terminal Phe. However, this appears unlikely as deamination of the N-terminal amino acid has never been observed in structurally characterized MBs from operons lacking *mbn*N (3, 5). The results suggest deamination of the N-terminal amino acid is not solely responsible for the 40 – 50nm absorption maxima difference between oxazolone groups in MBs. The absence of either the N-terminal or C-terminal oxazolone group in a small (0.5-2%) fraction of most MB-OB3b preparations (Fig. S3) also questions the suggestion that the absorption maxima difference between the N-terminal and C-terminal oxazolone groups is due solely to extending the conjugation of an additional double bond introduced following the deamination reaction.

The results presented here confirms MbnC is required for the formation of the C-terminal oxazolone group (Fig. 5). However, the results presented here also demonstrates MbnC is not required for the formation of the N-terminal oxazolone group in *M. trichosporium* OB3b suggesting the formation of the two hetercyclic groups with associated thioamides from XC dipeptides do not utilize the same enzyme(s). Future studies will determine if MbnB is involved in the formation of the N-terminal oxazolone, pyranzinedione or imidazolone groups. Resolution of the pathway and enzymes responsible for the post-translational modifications required for the synthesis of MB in methanotrophic bacteria will aid in the production of MBs derivatives with pharmacological properties specific for different metal-related diseases (19-24) as well as for environmental applications(10, 25).

MATERIALS AND METHODS

Bacterial strains, growth media, and culture conditions.

Plasmid construction was accomplished using *Escherichia coli* strain TOP10 (Invitrogen, Carlsbad, CA) as described previously (9). Plasmids used and constructed during this study are shown in Table 1. The donor strain for conjugation of plasmids into *Methylosinus trichosporium* OB3b was *E. coli* S17-1 (26). *E. coli* strains were cultivated at 37°C in Luria broth medium (Dot scientific, Burton, MI). Methanotrophic strains (i.e., *M. trichosporium* OB3b wildtype, *M. trichosporium* OB3b Δ*mbnAN*, *M. trichosporium* OB3b Δ*mbnC*, *Methylocystis* sp. strain SB2, and *Methylocystis parvus* OBBP) were cultivated at 30°C on nitrate mineral salts (NMS) medium (27), either in 250 ml flasks with side-arms at 200 rpm or in a 15-liter New Brunswick Bioflow 310 fermenter (Eppendorf, Hauppauge, NY,USA) using methane as the sole carbon and energy source. Where necessary, filter-sterilized solutions of copper (as $CuCl_2$) and spectinomycin were added to culture media aseptically. A working concentration of 20 $\mu g \bullet ml^{-1}$ spectinomycin was used for maintaining pWG104 in the *M. trichosporium* OB3b Δ *mbn*AN deletion mutant (i.e., *M. trichosporium* OB3b Δ*mbnC*). Chemicals were purchased from Fisher Scientific (Waltham, MA) or Sigma Aldrich (St. Louis, MO) with American Chemical Society reagent grade or better.

For ^{15}N NMR, $K^{14}NO_3$ in NMS media was replaced with $K^{15}NO_3$ (Cambridge Isotope Laboratories, Cambridge, MA, USA).

General DNA Methods, transformation and conjugation.

DNA purification and plasmid extraction were performed using QIAquick and QIAprep kits from Qiagen following the manufacturer's instruction. DNA cloning, preparation of chemically competent cells, and plasmid transformation with *E. coli* were performed according to (28) . Enzymes used for restriction digestion and ligation were purchased from New England Biolabs (Ipswich, MA). PCR of DNA for cloning purposes was accomplished using iProof-High Fidelity polymerase (Bio-Rad, Hercules, CA, USA). PCR for general purposes was accomplished using GoTaq DNA polymerase (Promega, Fitchburg, WI, USA). PCR programs were set according to manufacturers' suggestion. Plasmid pWG104 was conjugated into *M. trichosporium* OB3b Δ*mbnAN* with *E. coli* S17.1 as the donor strain as described by Martin and Murrell (29).

Construction of *M. trichosporium* OB3b Δ*mbnC* strain

Previously a mutant of *M. trichosporium* was constructed where *mbnABCMN* was deleted using a counter-selection technique (9). To characterize the function of *mbnC*, a Δ*mbnC* mutant was constructed by introducing pWG104 expression vector into the Δ *mbnAN* mutant. pWG104 was constructed by cloning two separate DNA fragments, one being a 1.9-kb DNA fragment of *mbnAB* (created via use of primers mbnANf and mbn66) and the other being a 2.5 DNA fragment of *mbnMN* (create via use of primers mbn70 and mbnANr), leaving out *mbnC*. These two fragments were amplified with BamHI restriction sites as indicated in Fig S2. These were then ligated together and cloned into the broad host range vector pTJS140 at the KpnI site.

Extraction of RNA and reverse transcription-PCR (RT-PCR)

244 To check the expression of genes restored to the *M. trichosporium* OB3b Δ*mbnC* mutant (e.g.
245 *mbnA*, *B, M* and *N*), genes associated with MB remaining in the chromosome (*mbnPH*), as well
246 as the absence of *mbnC*, RNA from the Δ*mbnC* mutant was collected, purified, and reverse
247 transcribed to cDNA to perform RT-PCR. Total RNA was isolated as described earlier (9). Briefly,
248 the Δ*mbnC* mutant was grown to the exponential phase, and RNA extracted using a phenol-
249 chloroform method modified from Griffiths *et al*. (30). Collected RNA was purified and removal
250 of DNA confirmed by the absence of 16S rRNA PCR product from PCR reactions. The same
251 amount of RNA (500ng) was used for reverse transcription by SuperScript III reverse
252 transcriptase (Invitrogen, Carlsbad, CA) for all reactions. RT-PCR analyses were performed to
253 confirm the expression of *mbnABMNPH* as well as the absence of *mbnC* using primers listed in
254 Table 1.
255
256 **Isolation of MB *from M. trichosporium* OB3b, *Methylocystis s*train SB2, *Methylocystis***
257 ***parvaus* OBBP and Δ*mbn*C.** MBs from all three methanotrophs were purified as previously
258 described (31).
259 **UV-visible absorption spectra.** UV-visible absorption spectra of $MbnC^{-}$, HPLC fractions
260 from MB preparations from *M. trichosporium* OB3b and *Methylocystis strain* SB2 and from the
261 MB from *M. parvus* OBBP were determined as previously describes (32, 33). Acid hydrolysis of
262 the oxazolone groups in the MB from *M. parvus* OBBP was carried out in 85µM acetic acid as
263 previously described (32)
264 **Structural Characterization of ΔMbnC**. UV-visible spectroscopy was recorded on a Cary
265 50 (Agilent, Santa Clara, CA, USA). Electrospray ionization (ESI)MS/MS was performed on an

Agilent LC using a Thermo Scientific Q Exactive Hybrid Quadrupole-Orbitrap Mass Spectrometer (Waltham, MA, USA) with an HCD fragmentation cell and an Agilent 1260 Infinity Capillary Pump with an Agilent Zorbax SB-C18, 0.5mm x 150mm, 5 micron, using 0.1% formic acid/water and 0.1% formic acid/acetonitrile as buffers A and B, respectively. NMR experiments were performed on a Bruker Advance 700 (Bruker Allentown PA, USA) with a Bruker 5 mm TCI 700 H/C/N cryoprobe or on a Bruker Advance 800 with a Bruker 5 mm TCI 800 H/C/N cryoprobe. NMR solutions were made using 15-40mg uniformly ^{15}N-MB-OB3b in a 90:10 H_20:D_2O mixture at pH 6.5. Unless otherwise specified, all experiments were run at 265 K and 3 kbar. Samples were placed in 3 kbar-rated sapphire NMR tubes (Daedalus Innovations LLC, Beverdam, VA, USA) and high pressure was generated by an Xtreme 60 (Daedalus Innovations). Analysis was performed in Mnova (Mestrelab Research, Escondido, CA, USA).

ACKNOWLEDGEMENTS

Funding: This research was supported by the U.S. Department of Energy Office of Science (Grants #DE-SC0018059 and DE-SC0020174; JDS and AAD), the National Science Foundation (Grant #1912482; JDS), the Roy J. Carver Charitable Trust (Muscatine, IA, USA) (JR) and the ISU Bailey Research and Career Development (TAB). Use of the Bruker Advance 800 was made possible through a generous gift from the Roy J. Carver Charitable Trust.

Competing interests: Authors declare they have no competing interests.

REFERENCES

1. DiSpirito AA, Semaru JD, Murrell JC, Gallagher WH, Dennison C, Vuilleumier S. 2016. Methanobactin and the link between copper and bacterial methane oxidation. Microbiol Mol Biol Rev 80:387-409.
2. El Ghazouani A, Basle A, Firbank SJ, Knapp CW, Gray J, Graham DW, Dennison C. 2011. Copper-binding properties and structures of methanobactins from *Methylosinus trichosporium* OB3b. Inorg Chem 50:1378-91.
3. El Ghazouani A, Basle A, Gray J, Graham DW, Firbank SJ, Dennison C. 2012. Variations in methanobactin structure influences copper utilization by methane-oxidizing bacteria. Proc Natl Acad Sci U S A 109:8400-4.
4. Kim HJ, Graham DW, DiSpirito AA, Alterman MA, Galeva N, Larive CK, Asunskis D, Sherwood PM. 2004. Methanobactin, a copper-acquisition compound from methane-oxidizing bacteria. Science 305:1612-5.
5. Krentz BD, Mulheron HJ, Semrau JD, DiSpirito AA, Bandow NL, Haft DH, Vuilleumier S, Murrell JC, McEllistrem MT, Hartsel SC, Gallagher WH. 2010. A comparison of methanobactins from *Methylosinus trichosporium* OB3b and *Methylocystis* strain SB2 predicts methanobactins are synthesized from diverse peptide precursors modified to create a common core for binding and reducing copper ions. Biochemistry 49:10117-10130.
6. Semau JD, DiSpirito AA, Obulisamy PK, Kang CS. 2020. Methanobactin from methanotrophs: genetics, structure, function and potential applications. FEMS Microbiol Lett 367:feaa045.
7. Semrau JD, DiSpirito AA, Gu W, Yoon S. 2018. Metals and Methanotrophy. Appl Environ Microbbiol 84:e02289-17.

8. Behling LA, Hartsel SC, Lewis DE, DiSpirito AA, Choi DW, Masterson LR, Veglia G, Gallagher WH. 2008. NMR, mass spectrometry and chemical evidence reveal a different chemical structure for methanobactin that contains oxazolone rings. J Am Chem Soc 130:12604-5.

9. Gu W, Baral BS, DiSpirito AA, Semrau JD. 2017. An aminotransferase is responsible for the deamination of the N-terminal leucine and required for formation of oxazolone ring A in Methanobactin of *Methylosinus trichosporium* OB3b. Appl Environ Microbiol 82:e01619-16.

10. Semrau JD, DiSpirito AA, Obulisamy PK, Kang-Yun CS. 2020. Methanobactin from methanotrophs: genetics, structure, function and potential applications. FEMS Microbiol Lett 367:fnaa045.

11. Kenney GE, Dassama LMK, Pandelia M-E, Gizzi AS, Martinie RJ, Gao P, DeHart CJ, Schachner LF, Skinner OS, Ro SY, Zhu X, Sadek M, Thomas PM, Almo SC, Bollinger MJ, Krebs C, Kelleher NL, Rosenzweig AC. 2018. The biosynthesis of methanobactin. Science 359:1411-1616.

12. Gu W, Farhan U-HM, Baral BS, Turpin EA, Bandow NL, DiSpirito AA, Lichtmannegger J, Kremmer E, Zischka H, Semaru JD. 2016. A TonB dependent transporter is responsible for methanobactin uptake by *Methylosinus trichosporium* OB3b. Appl Environ Microbiol 82:1917-1923.

13. Kenney GE, Rosenzweig AC. 2013. BMC Biol 11:17.

14. Chou JC-C, Strafford VE, Kenny GE, Dassama LMK. 2021. The enzymology of oxazolone and thioamide synthesis in Methanobactin. Meth Enzymol 656:341-373.

15. Choi DW, Do YS, Zea CJ, McEllistrem MT, Lee SW, Semrau JD, Pohl NL, Kisting CJ, Scardino LL, Hartsel SC, Boyd ES, Geesey GG, Riedel TP, Shafe PH, Kranski KA, Tritsch JR, Antholine WE, DiSpirito AA. 2006. Spectral and thermodynamic properties of Ag(I), Au(III), Cd(II), Co(II), Fe(III), Hg(II), Mn(II), Ni(II), Pb(II), U(IV), and Zn(II) binding by methanobactin from *Methylosinus trichosporium* OB3b. J Inorg Biochem 100:2150-61.

16. Eckert P, Jobs A, Semaru JD, DiSpirito AA, Richards J, Sarangi R, Herndon E, Gi B, Pierce EM. 2021. Spectroscopic and computational investigations of organometallic complexation of group 12 transition metals by methanobactins from *Methylocystis* sp. SB2. J Inorgan Biochem https://doi.org/10.1016/j.jinorgbio.2021.111496.

17. Bandow NL, Gallagher WH, Behling L, Choi DW, Semrau JD, Hartsel SC, Gilles VS, Dispirito AA. 2011. Isolation of methanobactin from the spent media of methane-oxidizing bacteria. Meth Enzymol 495:259-69.

18. Kenney GE, Goering AW, Ross MO, DeHart CJ, Thomas PM, Hoffman BM, Kelleher NL, Rosenzweig AC. 2016. Characterization of methanobactin from *Methylosinus* sp. SW4. J Am Chem Soc 138:11124 - 11127.

19. Zischka H, Lichmannnegger J, DiSpirito AA, Semrau JD. 2020. Methods and Means of Treating Copper Related Diseases. International.

20. Zischka H, Lichtmannegger J, Schmitt S, Jagemann N, Schulz S, Wartini D, Jennen L, Rust C, Larochette N, Galluzzi L, Chajes V, Bandow N, Gilles VS, DiSpirito AA, Esposito I, Goettlicher M, Summer KH, Kroemer G. 2011. Liver mitochondrial membrane crosslinking and destruction in a rat model of Wilson disease. J Clin Invest 121:1508-18.

21. Lichmannegger J, Leitinger C, Winner R, Schmitt S, Schulz S, Kabiri Y, Eberhagen C, Rieder T, Janik D, Neff F, Aichler M, DiSpirito AA, Bandow NL, Baral BS, Flatler A, Kremmer E, Denk G, Hohenester S, Eckardt-Schupp F, Dencher N, Adamski J, Merle U, Gotthardt DN, Kroemer G, Weiss KH, Zischka H. 2016. Methanobactin: a new effective treatment strategy against acute liver failure in a Wilson disease rat model. J Clin Inves 126:2721-2735.

22. Choi DW, Semrau JD, Antholine WE, Hartsel SC, Anderson RC, Carey JN, Dreis AM, Kenseth EM, Renstrom JM, Scardino LL, Van Gorden GS, Volkert AA, Wingad AD, Yanzer PJ, McEllistrem MT, de la Mora AM, DiSpirito AA. 2008. Oxidase, superoxide dismutase, and hydrogen peroxide reductase activities of methanobactin from types I and II methanotrophs. J Inorg Biochem 102:1571-80.

23. Summer KH, Lichtmannegger J, Bandow N, Choi DW, DiSpirito AA, Michalke B. 2011. The biogenic methanobactin is an effective chelator for copper in a rat model for Wilson disease. J Trace Elem Med Biol 25:36-41.

24. Mullert J-C, Lichtmannegger J, Zischka H, Sperling M, Karst U. 2018. High spatial resolution of LA-ICP-MS demonstrates massive liver copper depletion in Wilson disease rats upon methanobactin treatmenty. J Trace Elem Med Biol 49:119-127.

25. Lu X, Gu W, Zhao L, Fagan UHM, DiSpirito AA, Semrau JD, Gu B. 2017. Methylmercury uptake and degradation by methanotrophs. Science Adv 3:e1700041.

26. Simon R. 1984. High frequency mobilization of gram-negative bacterial replicons by the in vitro constructed Tn5-Mob transposon. Mol Gen Genet 196:413-420.

27. Whittenbury R, Phillips KC, Wilkinson JF. 1970. Enrichment, isolation and some properties of methane-utilizing bacteria. J Gen Microbiol 61:205-18.

28. Sambrook J, Russell DW. 2001. Molecular cloning: a laboratory manual 3rd edition. Coldspring-Harbor Laboratory Press, UK.
29. Martin H, Murrell JC. 1995. Methane monooxygenase mutants of *Methylosinus trichosporium* constructed by marker-exchange mutagenesis. FEMS Lett 127:243 - 248.
30. Griffiths RI, Whiteley AS, O'Donnell AG, Bailey MJ. 2000. Rapid method for coextraction of DNA and RNA from natural environments for analysis of ribosomal DNA-and rRNA-based microbial community composition. Appl Environ Microbiol 66:5488-5491.
31. Dershwiz P, Bandow NL, Yang J, Semaru JD, McEllistrem MT, Heinze RA, Fonseca M, Ledesma JC, Jennett JR, D'iSpirito AM, Athwal NS, Hargrove MS, Bobik TA, Zischka H, DiSpirito AA. 2021. Oxygen generation via water splitting by a novel biogenic metal ion binding compound. Appl Environ Microbiol 87:eoo286-21.
32. Bandow N, Gilles VS, Freesmeier B, Semrau JD, Krentz B, Gallaghe W, McEllistrem MT, Hartse SC, Cho DW, Hargrove MS, Heard TM, Chesner LM, Braunreiter KM, Cao BV, Gavitt MM, Hoopes JZ, Johnson JM, Polster EM, Schoenick BD, A.M. U, DiSpirito AA. 2012. Spectral and copper binding properties of methanobactin from the facultative methanotroph *Methylocystis* strain SB2. J Inorgan Biochem 110:72 - 82.
33. Choi DW, Zea CJ, Do YS, Semrau JD, Antholine WE, Hargrove MS, Pohl NL, Boyd ES, Geesey GG, Hartsel SC, Shafe PH, McEllistrem MT, Kisting CJ, Campbell D, Rao V, de la Mora AM, Dispirito AA. 2006. Spectral, kinetic, and thermodynamic properties of Cu(I) and Cu(II) binding by methanobactin from *Methylosinus trichosporium* OB3b. Biochemistry 45:1442-53.

34. Smith TJ, Slade SE, Burton NP, Murrell JC, Dalton H. 2002. Improved system for protein engineering of the hydroxylase component of soluble methane monooxygenase. Applied and environmental microbiology 68:5265-5273.

35. Semrau JD, Jagadevan S, DiSpirito AA, Khalifa A, Scanlan J, Bergman B, Freemeir BC, Baral BS, Bandow NL, Vorobev A, Haft DH, Vuilleumier S, Murrell JC. 2013. Methanobactin and MmoD work in concert to act as the “copper switch” in methanotrophs. Environ Microbiol 15:3077 - 3086.

Figure Legends

Fig. 1. UV-visible absorption spectra of MB-OB3b (blue) and ΔMbnC (red). Abbreviations; OxaA, oxazolone A or the N-terminal oxazolone group; OxaB, oxazolone B or the C-terminal oxazolone group.

Fig. 2. LC-ESI-MS of methanobactin from Δ*mbnC*.

Fig 3 (A) Structure of wild-type MB-OB3b, with the labile terminal methionine in gray. (B) Proposed structure of ΔMbnC based on UV-visible absorption spectra, LC-MS and NMR analysis, the differences between MB-OB3b-Met and ΔMbnC are highlighted in red. C. Amino acid sequence of (a) wild-type MB-OB3b minus the C-terminal Met and (b) ΔMbnC.

Fig. 4. 800 MHz (^{1}H,^{15}N)-HSQC spectrum of uniformly ^{15}N-labeled ΔMbnC in 90% 9 mM phosphate buffer, pH 6.5, and 10% D_2O at 265K and 3000 bar. The horizontal and vertical 1D spectra are ^{1}H and ^{15}N spectra, respectively.

Fig. 5. A. MB-OB3b gene cluster. Genes with known involvement in MB-OB3b synthesis and transport are shown in blue. B. Proposed genes involved in the biosynthesis of the oxazolones rings with associated thioamides from MbnA. Additional, yet to be identified genes may also be involved in the formation of oxazolone groups.

429 Table 1. Strains, plasmids, and primers used in this study.
430

Strains/Plasmids	Description	Restriction site	Reference/Source
Escherichia coli			
TOP10	F– *mcrA* Δ(*mrr-hsdRMS-mcrBC*) Φ80*lacZ*ΔM15 Δ*lacX74 recA1 araD139* Δ(*ara leu*) *7697 galU galK rpsL* (StrR) *endA1 nupG*		Invitrogen
S17.1 *λpir*	*recA1 thi pro hsdR*- RP4-2Tc::Mu Km::Tn*7* λ*pir*		(26)
Methylosinus trichosporium			
OB3b	Wild-type strain		
Δ*mbnAN*	*mbnABCMN* deleted		(9)
Δ*mbnC*	Δ*mbnAN* carrying pWG104		this study
Plasmids			
pTJS140	Broad-host-range cloning vector; Mob Ap^r Sp^r Sm^r *lacZ*		(34)
pWG104	pTJS140 carrying *mbnABMN* with its native promoter		this study
Primers			
mbnANf	ATTTTTggtaccGACGTTCGGGTCTTCTTCGC	KpnI	(9)
mbnANr	ATTTTTggtaccCGCCTCTAGATCATTCCGAC	KpnI	(9)
mbn66	ATTTTTggatccCGAACAATGTGTGCCAGTAG	BamHI	this study
mbn70	ATTTTTggatccGTTCGGCTATTTCCTGACGC	BamHI	this study
qmbnA_FO	TGGAAACTCCCTTAGGAGGAA		(35)
qmbnA_RO	CTGCACGGATAGCACGAAC		(35)
qmbnB_F1	TGGTCCAGCAGATGATCAAAG		this study
qmbnB_R2	TTCCCGAGCTTCTCCAATTC		this study
dmbnC_F	GGGAGAACAACCTCGCTTT		this study

dmbnC_R	CTTCCCAGCACGATCTGAC	this study
qmbnM_F	GCTAGGCTGGCTCCTTTATC	this study
qmbnM_R	GATGTTGACCACAAACCGAAAG	this study
qmbnN_F	CGATTCCATCCTTTCCGATGT	this study
qmbnN_R	CACTTTCGAAGACAAGGAGAGA	this study
qmbnP_F	AAAGGGAAGCACACACCCAT	this study
qmbnP_R	GTCGTGTTCTTGGCCGGATT	this study
qmbnH_F	ACTTACCGAAATACATCCCGC	this study
qmbnH_R	CGGAGAGGCGCTTATCGTAG	this study

434

435 **Table 2.** ^{1}H, ^{13}C, and ^{15}N resonances for metal free ΔMbnC.

Residue	Atom	Chemical Shifts (ppm) ^{1}H	^{13}C	^{15}N	Residue	Atom	Chemical Shifts (ppm) ^{1}H	^{13}C	^{15}N
3-Methyl-	C^{1}		174.6		Tyr[4]	H^{N}	7.44		
butanoyl	C^{2}		50.5			H^{α}	2.96		
	C^{3}		38.0			H^{β}	2.79		
	C^{4}		19.6			H^{β}	1.20		
	C^{5}		19.6			$H^{2,6}$	6.11		
	H^{2}	4.15				$H^{3,5}$	6.45		
	H^{3}	2.17			Pro[5]	N^{1}			109.6
	H^{3}	2.72				C^{2}		67.3	
	H^{4}	1.88				C^{3}		21.1	
	H^{5}	1.80				C^{4}		39.5	
Oxazolone	N			180.1		C^{5}		55.2	
	H^{N}	7.61				H^{2}	3.67		
Gly[1]	N			125.1		H^{3}	1.06		
	C					H^{3}	2.13		
	C^{α}		26.6			H^{4}	1.28		
	H^{N}	9.57				H^{4}	2.29		
	H^{α}	1.46				H^{5}	2.79		
Ser[2]	N			114.3		H^{5}	2.96		
	C		181.6		Cys[6]	N			127.9
	C^{α}		72			C		136.3	
	C^{β}					C^{α}		53.3	
	H^{N}	8.19				C^{β}		49.3	
	H^{α}	4.14				H^{N}	8.43		
	H^{β}	3.98				H^{α}	3.96		
	H^{β}	1.41				H^{β}	3.23		
Cys[3]	N			118.1		H^{β}	1.38		
	C		173.0		Ser[7]	N			117.5
	C^{α}		71.2			C			
	C^{β}		35.6			C^{α}		51.6	
	H^{N}	7.93				C^{β}		45.0	
	H^{α}	3.96				H^{N}	8.90		

	H^{β}	3.23				H^{α}	4.19		
	H^{β}	1.37				H^{β}	3.25		
Tyr^{4}	N			121.5		H^{β}	1.48		
	C				Cys^{8}	N			112.4
	C^{α}		48.9			C		172.6	
	C^{β}		35.6			C^{α}		42.3	
	C^{1}					C^{β}		21.1	
	$C^{2,6}$					H^{N}	8.47		
	$C^{3,5}$		135.4			H^{α}	3.69		
	C^{4}					H^{β}	3.55		
						H^{β}	0.97		

436

437

438

Table 2. ^{1}H, ^{13}C, and ^{15}N resonances for metal free ΔMbnC.

Residue	Atom	Chemical Shifts (ppm) ^{1}H	^{13}C	^{15}N	Residue	Atom	Chemical Shifts (ppm) ^{1}H	^{13}C	^{15}N
3-Methyl-	C^{1}		174.6		Tyr^{4}	H^{N}	7.44		
butanoyl	C^{2}		50.5			H^{α}	2.96		
	C^{3}		38.0			H^{β}	2.79		
	C^{4}		19.6			H^{β}	1.20		
	C^{5}		19.6			$H^{2,6}$	6.11		
	H^{2}	4.15				$H^{3,5}$	6.45		
	H^{3}	2.17			Pro^{5}	N^{1}			109.6
	H^{3}	2.72				C^{2}		67.3	
	H^{4}	1.88				C^{3}		21.1	
	H^{5}	1.80				C^{4}		39.5	
Oxazolone	N			180.1		C^{5}		55.2	
	H^{N}	7.61				H^{2}	3.67		
Gly^{1}	N			125.1		H^{3}	1.06		
	C					H^{3}	2.13		
	C^{α}		26.6			H^{4}	1.28		
	H^{N}	9.57				H^{4}	2.29		
	H^{α}	1.46				H^{5}	2.79		
Ser^{2}	N			114.3		H^{5}	2.96		
	C		181.6		Cys^{6}	N			127.9
	C^{α}		72			C		136.3	
	C^{β}					C^{α}		53.3	
	H^{N}	8.19				C^{β}		49.3	
	H^{α}	4.14				H^{N}	8.43		
	H^{β}	3.98				H^{α}	3.96		
	H^{β}	1.41				H^{β}	3.23		
Cys^{3}	N			118.1		H^{β}	1.38		
	C		173.0		Ser^{7}	N			117.5
	C^{α}		71.2			C			
	C^{β}		35.6			C^{α}		51.6	
	H^{N}	7.93				C^{β}		45.0	
	H^{α}	3.96				H^{N}	8.90		
	H^{β}	3.23				H^{α}	4.19		
	H^{β}	1.37				H^{β}	3.25		

Tyr^4	N		121.5		H^{β}	1.48	
	C			Cys^8	N		112.4
	C^{α}	48.9			C	172.6	
	C^{β}	35.6			C^{α}	42.3	
	C^1				C^{β}	21.1	
	$C^{2,6}$				H^N	8.47	
	$C^{3,5}$	135.4			H^{α}	3.69	
	C^4				H^{β}	3.55	
					H^{β}	0.97	

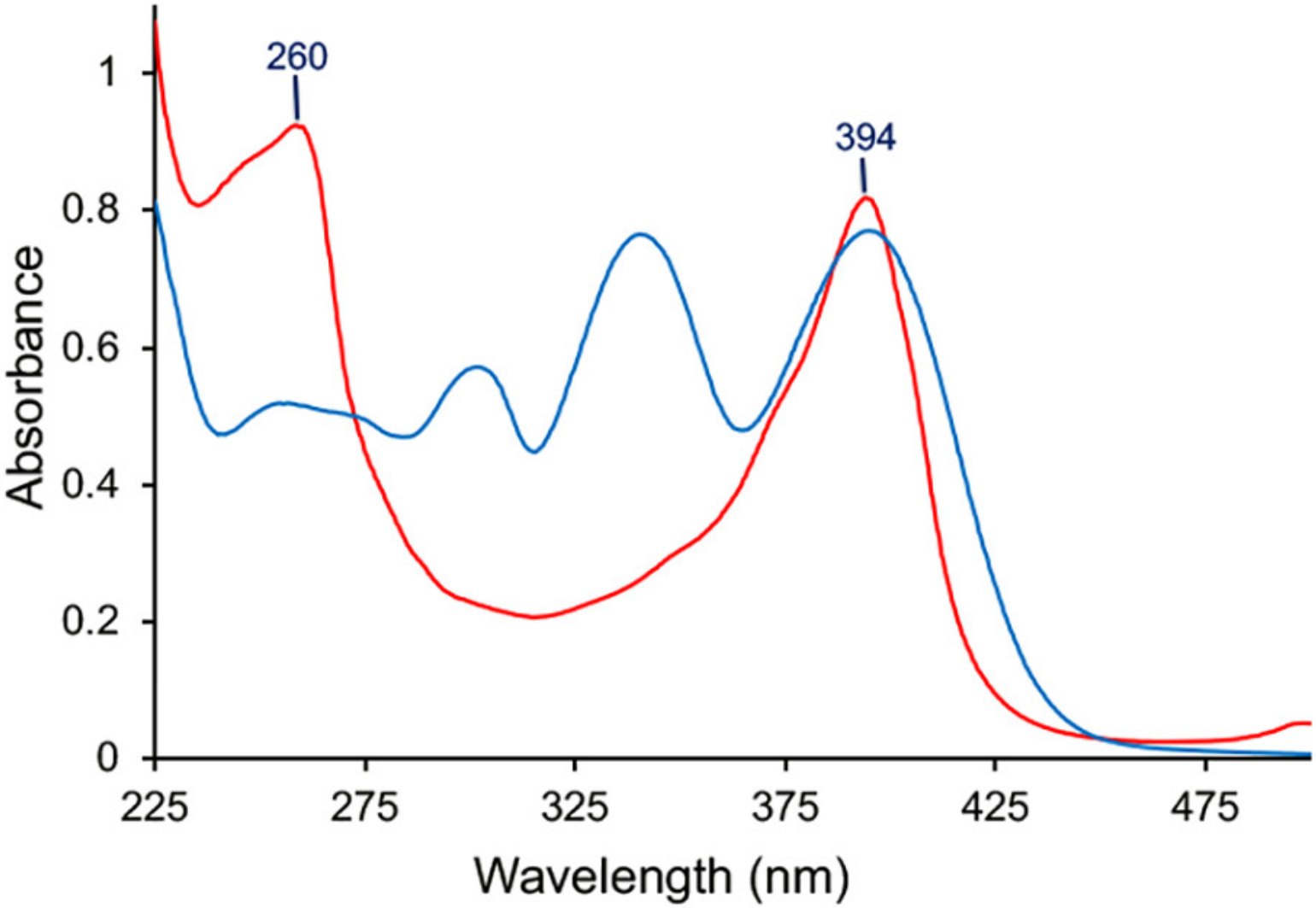
260
394
1
0.8
0.6
0.4
0.2
0
Absorbance
225
275
325
375
425
475
Wavelength (nm)

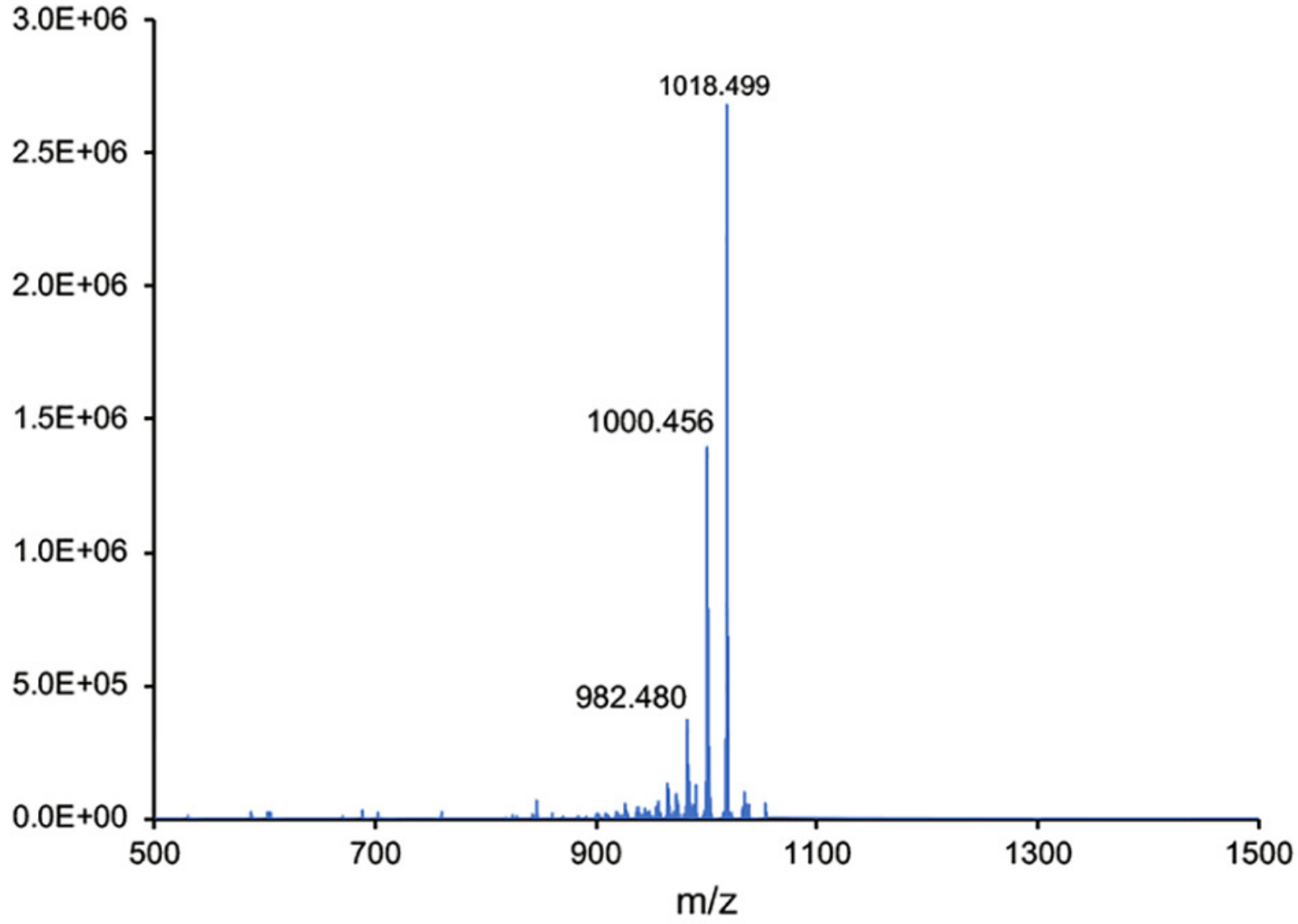
3.0E+06
2.5E+06
2.0E+06
1.5E+06
1.0E+06
5.0E+05
0.0E+00
1018.499
1000.456
982.480
500
700
900
1100
1300
1500
m/z

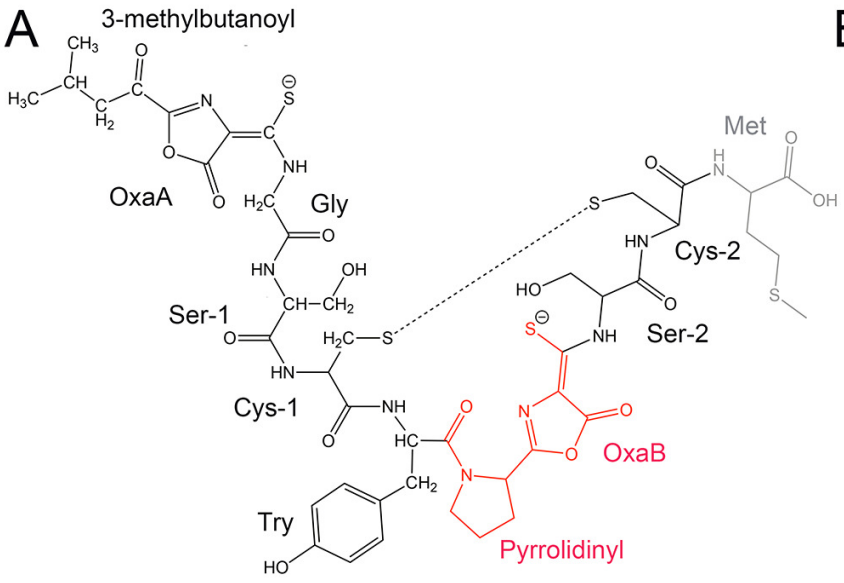
A
3-methylbutanoyl
OxaA
Gly
Ser-1
Cys-1
Try
Pyrrolidinyl
OxaB
Cys-2
Ser-2
Met

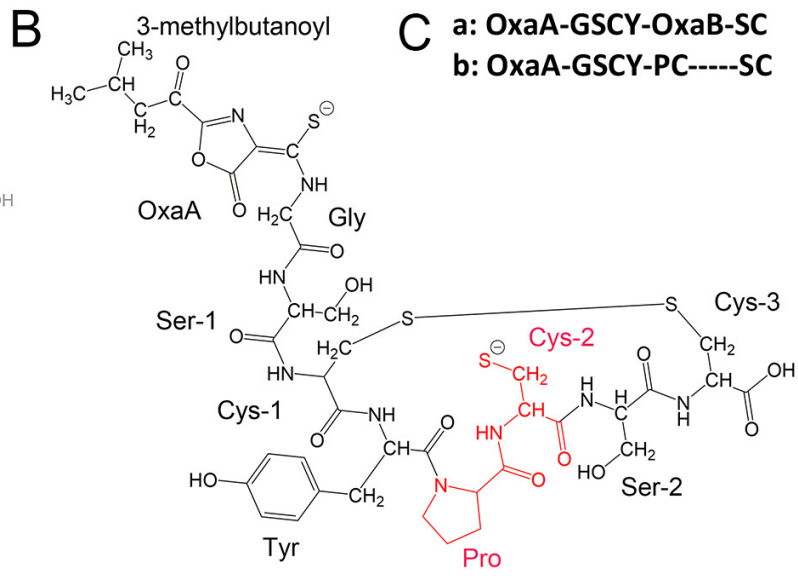
B
3-methylbutanoyl
OxaA
Gly
Ser-1
Cys-1
Tyr
Pro
Cys-2
Cys-3
Ser-2
C
a: OxaA-GSCY-OxaB-SC
b: OxaA-GSCY-PC-----SC

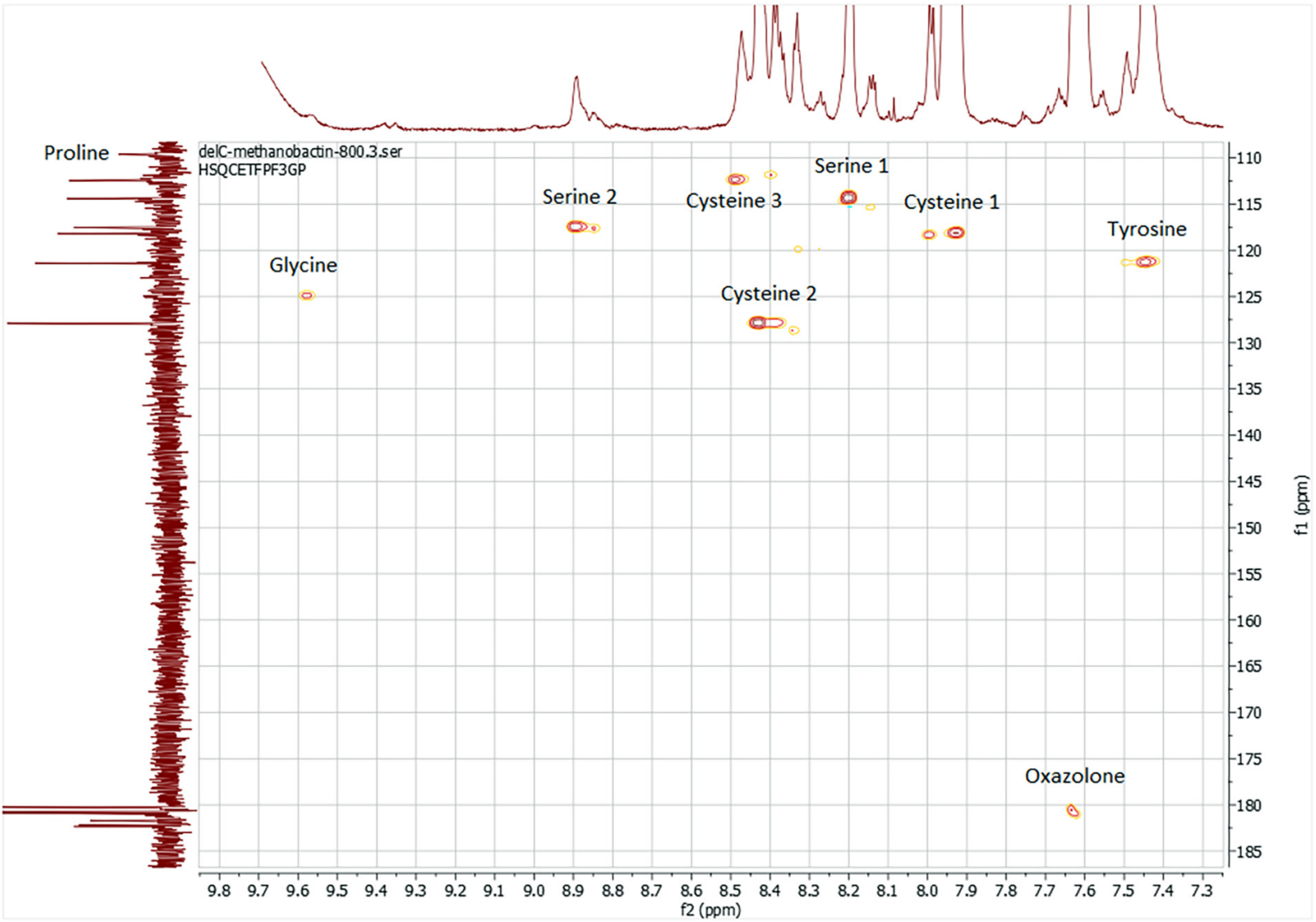
delC-methanobactin-800.3.ser
HSQCETFPF3GP
Proline
Glycine
Serine 2
Cysteine 3
Serine 1
Cysteine 1
Tyrosine
Cysteine 2
Oxazolone
f2 (ppm)
f1 (ppm)

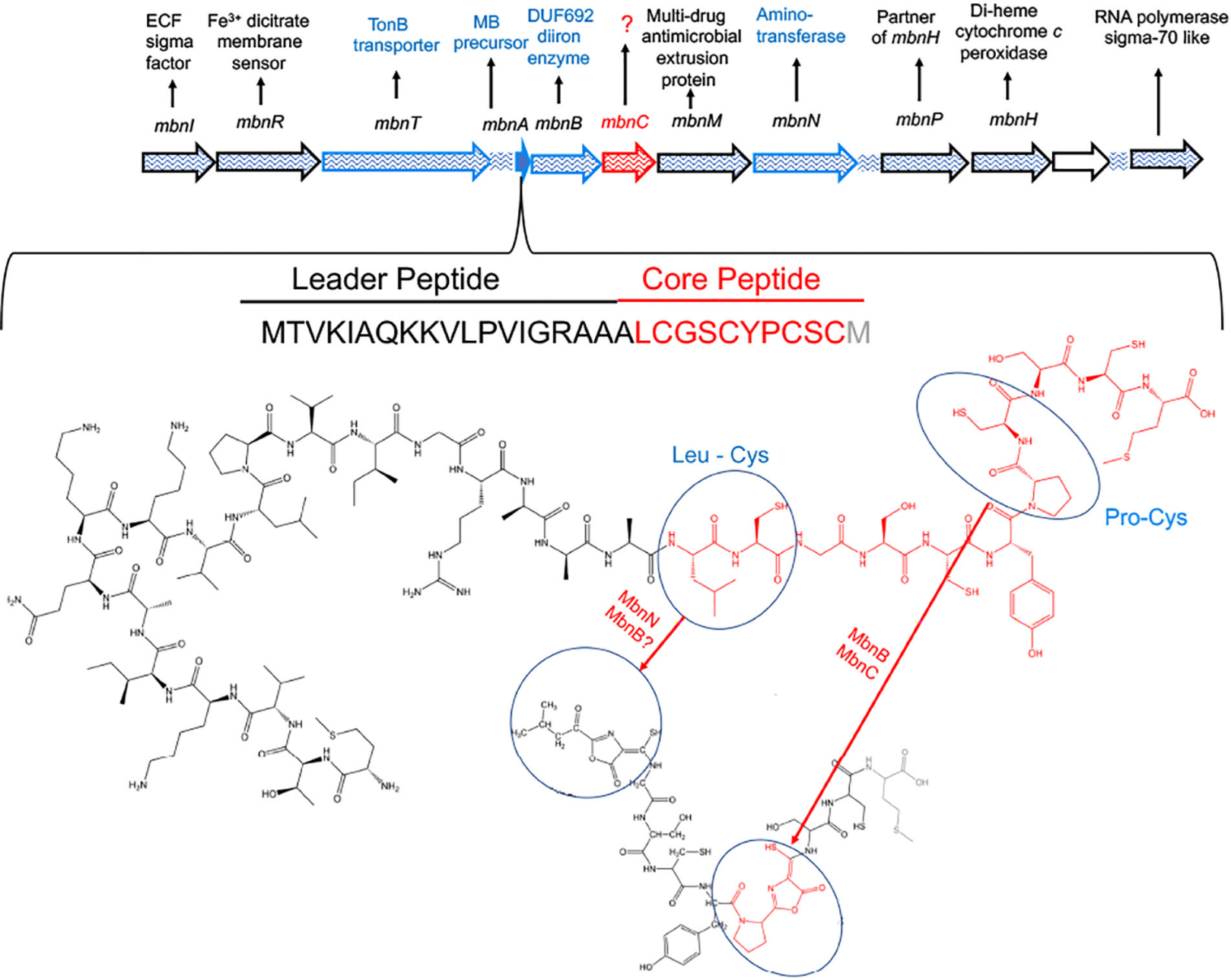
ECF sigma factor
Fe3+ dicitrate membrane sensor
TonB transporter
MB precursor
DUF692 diiron enzyme
?
Multi-drug antimicrobial extrusion protein
Amino-transferase
Partner of mbnH
Di-heme cytochrome c peroxidase
RNA polymerase sigma-70 like
mbnI
mbnR
mbnT
mbnA
mbnB
mbnC
mbnM
mbnN
mbnP
mbnH
Leader Peptide
Core Peptide
MTVKIAQKKVLPVIGRAAALCGSCYPCSCM
Leu - Cys
Pro-Cys
MbnN
MbnB?
MbnB
MbnC